ISSN 1810-2328, Journal of Engineering Thermophysics, 2024, Vol. 33, No. 4, pp. 883–900. © Pleiades Publishing, Ltd., 2024.

Insights into Significance of Radiative Inclined MHD on Mixed Convective Viscoelastic Flow of Hybrid Nanofluid over a Permeable Surface with Mass Transpiration

G. M. Sachin[1*], T. Maranna[1], U. S. Mahabaleshwar[1***], L. M. Pérez[2****], D. Laroze[3*****], and G. Lorenzini[4******]**

[1] *Department of Studies in Mathematics, Davangere University, Shivagangothri, Davangere, 577 007, India*

[2] *Departamento de Ingeniería Industrial y de Sistemas, Universidad de Tarapacá, Casilla 7D, Arica 1000000,Chile*

[3] *Instituto de Alta Investigación, Universidad de Tarapacá, Casilla 7D, Arica 1000000, Chile*

[4] *Università degli Studi di Parma, Dipartimento di Ingegneria e Architettura, Parma, Italy*

Received August 5, 2024; in final form, October 23, 2024; accepted October 24, 2024

Abstract—The hybrid nanofluid is extensively used in manufacturing for industrial uses because of its exceptional property of enhancing the heat transfer process. The purpose of the present work is to find novel explanations for the behavior of thermal radiation and inclined magnetohydrodynamics effects on the convective viscoelastic flow of water Al_2O_3–Cu hybrid nanofluids over an accelerating permeable surface with mass transpiration. The viscoelastic liquid concept is postulated with the benefit of hybrid nanofluids employing conventional flow patterns that are impacted by the magnetic field. Thermophysical properties of Al_2O_3–Cu and water are employed. Nonlinear PDE for momentum, temperature, and concentration are converted into non-dimensional ODE by employing the proper similarity transformations. The current study is reported to be in very good accordance with earlier research. The velocity field and energy distributions were depicted graphically to show the influence and typical behaviors of physical factors such as the viscoelastic parameter, the Richardson number, the radiation number, etc. In industrial applications, the temperature distribution influenced by radiation is quite important, specifically in accelerated plates where cooling the liquid is necessary to achieve the desired outcome.

DOI: 10.1134/S1810232824040179

1. INTRODUCTION

Heat transfer, which is performed through heat transfer in single- as well as multiphase flow scenarios, is one of the most essential manufacturing applications. Despite the fact that there have been well-developed and incorporated theoretical models for heat transfer since the 1970s, there has been a great deal of interest and effort put into innovative research in this area because of the requisite need and strong demand for industrial uses that necessitate the enhancement and design of heat exchangers. The rate of heat transfer has been improved in recent years through a variety of means, one of which is improving the thermal conductivity. Choi [1] was a pioneer in developing nanofluid as well as its capacity to sustain nanoscale particles in the base fluid because they have improved thermal conductivity and a larger efficiency of convective heat transfer. Nanoparticles are a remarkable accomplishment for a variety of industrial purposes, including microelectronics, hybrid-powered engines, household refrigerators, chillers, and even highly functional military specialist

[*] E-mail: sgmwithusm@gmail.com
[**] E-mail: marannat4@gmail.com
[***] E-mail: u.s.m@davangereuniversity.ac.in
[****] E-mail: lperez@academicos.uta.cl
[*****] E-mail: dlarozen@uta.cl
[******] Corresponding author. E-mail: giulio.lorenzini@unipr.it

equipment. However, a novel nanofluid known as hybrid nanofluid is being researched, and the rate of heat transport should be increased. While conventional nanofluids only possess a unique nanoparticle that dissolves in the base fluid, hybrid nanofluids are upgraded nanofluids that contain two different nanoparticles.

Hybrid nanofluid provides improved thermophysical properties, increasing heat transmission efficiency. Researchers who have started to investigate HNF in solar radiation have found a new dawn in hybrid nanofluids due to their thermal properties. Numerous fields of study [2, 3] have greatly benefited from the examination of mathematical modeling's outputs of natural phenomena. Studies on thermal absorption or the production of HNF are extensive, and numerous researchers have worked to understand this interesting behavior. Over the past decade, the number of studies on nanofluids has grown significantly, in research by Sarkar et al. [4] studied that the hybrid nanofluids thermal performance is better addressed by using the appropriate hybridization approach. The role of Cu/H_2O HNF in the permeable stretched sheet was the subject of research by Devi et al. [5].

Mahabaleshwar et al. [6–10] studied on the flow of HNF past a stretching/shrinking surface in permeable media along the influence of radiations and magnetohydrodynamic slip along temperature and concentration conditions. Illustrations of mixed convection flows include the flow changes in the ocean and atmosphere, wind-swept solar receivers, electrical equipment refrigerated by fans, and other thermal changes in the atmospheric circulation. Researchers have widely pondered about what flows over an extending surface: boundary layer heat and mass convections due to consistently but differing heat as well as mass across borders. [11, 12] developed the exact solutions for magnetohydrodynamic viscoelastic flow of mixed convection liquid due to a porous stretched sheet. By using a vertically porous stretchable plate enclosed in a porous material.

A quantitative approach to the H_2O-based nanofluid flow impacted by an applied Lorentz force was used by Ferdows et al. [13]. Waini et al. [14] revealed a hybrid nanofluid is used to model the coupled convection flow and heat along a vertical plane that is gradually expanding or contracting. A numerical analysis is conducted to determine how viscous dissipation and thermophoretic influence radiative combined convection, which incorporates HNF, around an inclined porous sliding flat disk with force field was discussed by Khan et al. [15]. Casson fluid flowing in magnetohydrodynamic mixed convection over a prolonged surface, although Hall as well as thermal radiation impacts are present, assessment is accomplished by Ashraf et al. [16].

Viscoelastic fluid is an example of a non-Newtonian liquid subclasses. Due to its numerous uses in air container, production of petroleum along with the manufacture of complicated multistage commodities like dyes, inks, as well as ceramic pastes. Researchers [17–20] recently conducted significant study to investigate the viscoelastic fluid flow in response to an external magnetic force with heat source/sink while taking into account a variety of flow conditions. This study was inspired by potential industrial uses.

2. DEVELOPMENT OF PROBLEM

In the present study, the steady laminar 2D thermally radiated mixed convection inclined magnetohydrodynamic hybrid nanofluid Al_2O_3–Cu flow across a porous stretching surface. Here x-axis is directed and y- axis upward direction to sheet. Temperature and concentration are takes the constant values T_w and C_w, constant values T_∞ and C_∞. The schematic representation of the flow problem is shown in Fig. 1.

The governing equations are [11, 21]

$$\frac{\partial u}{\partial x}+\frac{\partial v}{\partial y}=0, \tag{1}$$

$$u\frac{\partial u}{\partial x}+v\frac{\partial u}{\partial y}=\frac{\mu_{hnf}}{\rho_{hnf}}\frac{\partial^2 u}{\partial y^2}-k_0\left(u\frac{\partial^3 u}{\partial x\partial y^2}+\frac{\partial u}{\partial x}\frac{\partial^2 u}{\partial y^2}+\frac{\partial u}{\partial y}\frac{\partial^2 v}{\partial y^2}+v\frac{\partial^3 u}{\partial y^3}\right)-\frac{\mu_{hnf}}{\rho_{hnf}K}u$$

$$-\frac{\sigma_{hnf}B_0^2\sin^2\tau}{\rho_{hnf}}u+g\left\{\beta_T\left(T-T_\infty\right)+\beta_c\left(C-C_\infty\right)\right\}=0, \tag{2}$$

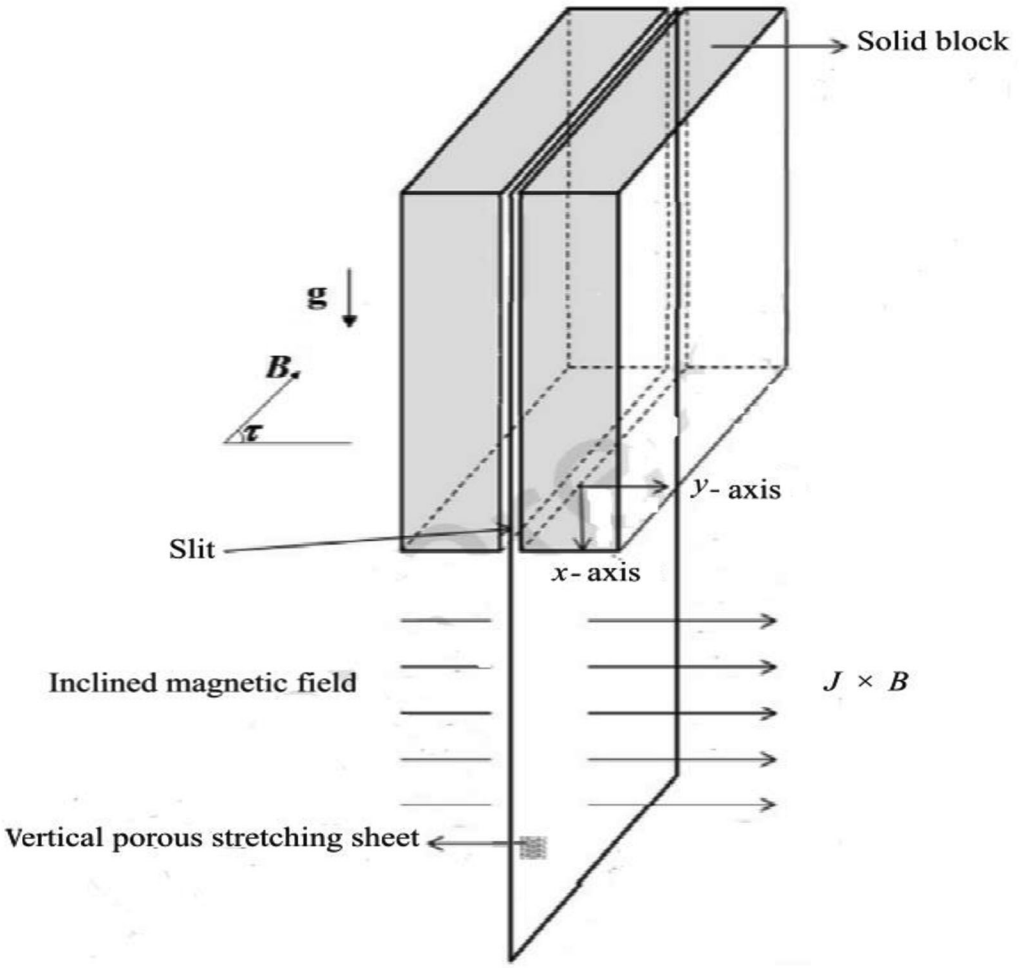

Fig. 1. Schematic representation of flow problem.

$$u\frac{\partial T}{\partial x}+v\frac{\partial T}{\partial y}=\frac{\kappa_{hnf}}{(\rho C_p)_{hnf}}\frac{\partial^2 T}{\partial y^2}+\frac{D_m K_T}{C_p C_s}\frac{\partial^2 C}{\partial y^2}-\frac{1}{(\rho C_p)_{hnf}}\frac{\partial q_r}{\partial y}, \tag{3}$$

$$u\frac{\partial C}{\partial x}+v\frac{\partial C}{\partial y}=D_m\frac{\partial^2 C}{\partial y^2}+\frac{D_m K_T}{T_m}\frac{\partial^2 T}{\partial y^2}, \tag{4}$$

where k_0 be the viscoelastic factor. Permeability is denoted as K, dynamic viscosity or absolute viscosity is μ_{hnf}, ρ_{hnf} is the density, electrical conductivity of hybrid nanofluid is defined as σ_{hnf}, the thermal conductivity is represented to be κ_{hnf}, and $(\rho C_p)_{hnf}$ is the HNFs specific heat with other physical parameter mentioned in the nomenclature.

The current study considers the following boundary constraints are

$$u=U_w(x)=ax,\quad v=v_c,\quad T=T_w(x)=T_\infty+bx,\quad C=C_w(x)=C_\infty+cx \qquad \text{at } y=0,$$

$$u\to 0,\quad \frac{\partial u}{\partial y}\to 0,\qquad T\to T_\infty,\qquad C\to C_\infty \qquad \text{at } y\to\infty. \tag{5}$$

Velocity of mass flux is v_c together with for suction $v_c>0$ for suction and $v_c<0$ for injection. Additionally, fluid temperature is denoted as T, T_∞ be the ambient temperature of the fluid. Further a, b with c are constants.

Let's assume the similarity transformations to simplified the governed equations to non-dimensional ordinary differential equations as

$$u = axf'(\eta), \quad v = -\sqrt{av_f} f(\eta), \quad \eta = \sqrt{\frac{a}{v_f}} y,$$

$$\theta(\eta) = \frac{T - T_\infty}{T_w - T_\infty}, \qquad \varphi(\eta) = \frac{C - C_\infty}{C_w - C_\infty}. \tag{6}$$

Here wall concentration is C_w, with concentration gradient as denoted as C_∞, v_f is the kinematic viscosity of the base fluid.

Radiative heat flux q_r is represented using Roselands approximation [22–25].

$$q_r = -\frac{4\sigma^*}{3k^*}\frac{\partial T^4}{\partial y}, \tag{7}$$

where σ^* and k^* are Stefan–Boltzmann, and absorption factors. we elaborate T^4 in Taylor's series about T_∞ we get.

$$T^4 = T_\infty^4 + 4T_\infty^3 (T - T_\infty) + 6T_\infty^2 (T - T_\infty)^2 + \ldots \tag{8}$$

Ignoring higher order components following the first degree $(T - T_\infty)$, we may suppose

$$T^4 \approx 3T_\infty^4 + 4T_\infty^3 T. \tag{9}$$

Differentiate Eq. (7) in relation to y with substitute Eq. (9) we get

$$\frac{\partial q_r}{\partial y} = -\frac{16T_\infty^3\sigma^*}{3k^*}\frac{\partial^2 T}{\partial y^2}. \tag{10}$$

Using Eq. (10) in Eq. (3) we obtain

$$u\frac{\partial T}{\partial x} + v\frac{\partial T}{\partial y} = \left(\frac{\kappa_{hnf}}{(\rho C_p)_{hnf}} + \frac{16\sigma^* T_\infty^3}{3k^*(\rho C_p)_{hnf}}\right)\frac{\partial^2 T}{\partial y^2} + \frac{D_m K_T}{C_p C_s}\frac{\partial^2 C}{\partial y^2}. \tag{11}$$

Employing the Eq. (6), Eqs. (2), (3) and boundary condition (5) are modified to the following ODEs:

$$\frac{A_1}{A_2}\frac{d^3 f}{d\eta^3} + f(\eta)\frac{d^2 f}{d\eta^2} - \left(\frac{df}{d\eta}\right)^2 + K_1\left\{f(\eta)\frac{d^4 f}{d\eta^4} - 2\frac{df}{d\eta}\frac{d^3 f}{d\eta^3} + \left(\frac{d^2 f}{d\eta^2}\right)^2\right\}$$

$$-\left\{\frac{A_1}{A_2}Da^{-1} + \frac{A_3}{A_2}QB_0^2\sin^2\tau\right\}\frac{df}{d\eta} + \Lambda\{\theta(\eta) + N\varphi(\eta)\} = 0, \tag{12}$$

$$\left(\frac{A_4}{A_5} + \frac{N_r}{A_5}\right)\frac{d^2\theta}{d\eta^2} + \Pr\left\{f(\eta)\frac{d\theta}{d\eta} - \frac{df}{d\eta}\theta(\eta) + D_f\frac{d^2\varphi}{d\eta^2}\right\} = 0, \tag{13}$$

$$\frac{d^2\varphi}{d\eta^2} + Le\left\{\Pr\left(f(\eta)\frac{d\varphi}{d\eta} - \frac{df}{d\eta}\varphi(\eta)\right) + S_r\frac{d^2\theta}{d\eta^2}\right\} = 0, \tag{14}$$

Table 1. Thermophysical properties of HNFs [26–30]

Properties of Hybrid nanofluid
Density
$\rho_{hnf} = (1-\phi_2)\left[(1-\phi_1)\rho_f + \rho_{s1}\right] + \phi_{s2}$
Heat capacity
$(\rho C_p)_{hnf} = (1-\phi_1)\left[(1-\phi_1)(\rho C_p)_f + \phi_1 (\rho C_p)_{s1}\right] + \phi_2 (\rho C_p)_{s2}$
Dynamic viscosity
$\mu_{hnf} = \dfrac{\mu_f}{(1-\phi_1)^{2.5}(1-\phi_2)^{2.5}}$
Thermal conductivity
$\kappa_{hnf} = \dfrac{\kappa_f(\kappa_{s2}+2\kappa_{bf}+2\phi_2(\kappa_{s2}-\kappa_f))}{(\kappa_{s2}+2\kappa_{bf}-(\kappa_{s2}-\kappa_f))}$, where $\kappa_{bf} = \dfrac{\kappa_f(\kappa_{s1}+\kappa_f+2\phi_1(\kappa_{s1}-\kappa_f))}{(\kappa_{s1}+2\kappa_f-(\kappa_{s1}-\kappa_f))}$
Electrical conductivity
$\sigma_{hnf} = \dfrac{\sigma_{s2}+2\sigma_{nf}-2\phi_2(\sigma_{nf}-\sigma_{s2})}{\sigma_{s2}+2\sigma_{nf}+2\phi_2(\sigma_{nf}-\sigma_{s2})} * \sigma_f$, where $\sigma_{nf} = \dfrac{\sigma_{s1}+2\sigma_f-2\phi_1(\sigma_f-\sigma_{s1})}{\sigma_{s1}+2\sigma_f+\phi_1(\sigma_f-\sigma_{s1})} * \sigma_f$

Table 2. Thermophysical properties [26, 31–33]

Properties	Al_2O_3	Cu	Base fluid (water)
ρ (kg/m^3)	3970	8933	997.1
C_p (J/kgK)	765	385	4179
κ (W/mK)	40	401	0.613
σ (s/m)	3.69×10^7	5.96×10^7	0.05

where $A_1 = \frac{\mu_{hnf}}{\mu_f}$, $A_2 = \frac{\rho_{hnf}}{\rho_f}$, $A_3 = \frac{\sigma_{hnf}}{\sigma_f}$, $A_4 = \frac{\kappa_{hnf}}{\kappa_f}$, and $A_5 = \frac{(\rho C_p)_{hnf}}{(\rho C_p)_f}$. Also $Da^{-1} = \frac{\nu_f}{Ka}$ is the Darcy number, Hartmann number is defined as $Q = \frac{\sigma_f B_0^2}{\rho_f a}$, $\Lambda = \frac{Gr_x}{\mathrm{Re}_x^2}$ denotes Richardson number, whereas $Gr_x = \frac{g\beta_T(T_w - T_\infty)x^3}{\nu_f}$ known as local Grashof number with $\mathrm{Re}_x = \frac{u_w(x)x}{\nu_f}$ being local Reynolds number. $K_1 = \frac{k_0 a}{\nu_f}$ be the viscoelastic parameter, and $K_1 > 0$ denotes the Walter's liquid B and commonly known as second order fluid. $N = \frac{\beta_c C_w - C_\infty}{\beta_T T_w - T_\infty}$ is represented as the concentration buoyancy parameter, moreover characteristics of Prandtl number is denoted by $\mathrm{Pr} = \frac{\kappa_f}{(\rho C_p)_f \nu_f}$, Dufour number is $D_f = \frac{D_m K_T}{\nu_f C_s C_p}\frac{C_w - C_\infty}{T_w - T_\infty}$. Soret number is estimated as $Sr = \frac{D_m K_T}{\nu T_m}\frac{T_w - T_\infty}{C_w - C_\infty}$, additionally, $Le = \frac{\alpha}{D_m}$ to be Lewis number and $N_r = \frac{16\sigma^* T_\infty^3}{3k^*\kappa_f}$ is the radiation parameter.

With proper subjected to the boundary constraints,

$$\left(\frac{df}{d\eta}\right)_{\eta=0} = 1, \quad f(\eta)_{\eta=0} = V_c, \quad \theta(\eta)_{\eta=0} = 1, \quad \varphi(\eta)_{\eta=0} = 1,$$

$$\left(\frac{df}{d\eta}\right)_{\eta\to\infty} = 0, \quad \theta(\eta)_{\eta\to\infty} \to 0, \quad \varphi(\eta)_{\eta\to\infty} \to 0. \tag{15}$$

3. ANALYTICAL SOLUTION FOR THE PROBLEM MOMENTUM

An exact solution to Eqs. (12)–(14) with associated dimensionless boundary conditions (15) is given by the similarity transformation

$$f(\eta) = V_c + \frac{1 - e^{-\beta\eta}}{\beta}, \tag{16}$$

with derivative of Eq. (16) written as

$$\frac{\partial f}{\partial \eta} = e^{-\beta\eta} = \theta(\eta) = \varphi(\eta), \tag{17}$$

now substitute Eqs. (16), (17) in Eqs. (12)–(14). We have

$$\left(\frac{A_1}{A_2} - K_1\right)\beta^2 - \beta V_c\left(1 + K_1\beta^2\right) + \left\{\Lambda(1+N) - \left(\frac{A_1}{A_2}Da^{-1} + \frac{A_3}{A_2}Q\sin^2\tau + 1\right)\right\} = 0, \tag{18}$$

$$\left(\frac{A_4}{A_5} + \frac{N_r}{A_5}\right)\beta^2 + \Pr\left(D_f\beta^2 - V_c\beta - 1\right) = 0, \tag{19}$$

$$\beta^2 - Le\left\{\Pr - \Pr V_c - Sr\beta^2\right\} = 0. \tag{20}$$

In order to rearranged Eqs. (18), (19), we obtained modified equation can be written as in terms of β, where β is the real root of the following biquadratic polynomial equation:

$$\left(\frac{A_4}{A_5} + \frac{N_r}{A_5}\right)K_1\beta^2 + \left\{\left(\frac{A_4}{A_5} + \frac{N_r}{A_5}\right) - \left(\frac{A_1}{A_2} - K_1\right)\Pr\right\}\beta^2$$
$$+ \left\{\Lambda(1+N) - \left(\frac{A_1}{A_2}Da^{-1} + \frac{A_3}{A_4}Q\sin^2\tau\right)\right\}\Pr = 0. \tag{21}$$

The above equation we rewritten as

$$\xi_1 K_1\beta^4 + \xi_2\beta^2 + \Gamma\Pr = 0, \tag{22}$$

where $\xi_1 = \left(\frac{A_4}{A_5} + \frac{N_r}{A_5}\right)$, $\xi_2 = \left(\frac{A_4}{A_5} + \frac{N_r}{A_5}\right) - \left(\frac{A_1}{A_2} - K_1\right)\Pr$, and

$$\Gamma = \Lambda(1+N) - \left(\frac{A_1}{A_2}Da^{-1} + \frac{A_3}{A_2}Q\sin^2\tau\right),$$

Eq. (22) gives four real roots, consequently, the four solutions are

$$\beta_{1,2} = \pm\frac{\sqrt{-\frac{\xi_2}{\xi_1 K_1} - \frac{\sqrt{\xi_2^2 - 4\xi_1 K_1\Pr\Gamma}}{\xi_1 K}}}{\sqrt{2}},$$

$$\beta_{3,4} = \pm\frac{\sqrt{-\frac{\xi_2}{\xi_1 K_1} + \frac{\sqrt{\xi_2^2 - 4\xi_1 K_1\Pr\Gamma}}{\xi_1 K}}}{\sqrt{2}}. \tag{23}$$

In order to solve Eqs. (19), (20), we have the value of the Prandtl number

$$\Pr = \frac{Le\left\{Sr - \left(\frac{A_4}{A_5} + \frac{N_r}{A_5}\right)\right\} + 1}{Le\, D_f}, \tag{24}$$

particularly important to observe that Eq. (24) imposes limitation on the Prandtl number, which is always pragmatic. With other perspective, there are wide range of parameters Le, Sr, and D_f for a given value of Pr.

4. INTERPRETATION OF RESULT

The behavior of inclined MHD mixed convection flow for viscoelastic hybrid nanoliquid impacted by thermal radiation and mass transpiration is investigated. Al_2O_3–Cu solid nanoparticles, together H_2O considered to be base liquid. The base fluid dissolves the solid particles, yielding the hybrid nanoparticle. We illustrate Dufour as well as Soret consequences non-Newtonian liquid movement caused by an accelerated surface. Equations (12)–(14) are solved analytically. The pictorial results of dimensionless parameters are displayed in this part. The current work findings are verified with the existing results by considering $\phi = 0$, indicates the absence of nanoparticles as well as $\phi \neq 0$, indicates the presence of nanofluid. Graphical depictions were utilized to analyze the impacts of the pertinent parameters, namely, radiation parameter, Richardson number, Hartmann number, Mass transpiration parameter, and viscoelastic parameter etc. Thermophysical properties and numerical quantities of HNFs are mentioned in Tables 1 and 2.

Figures 2a, b show how different profiles are affected by thermal radiation parameters for second grade fluid with $\tau = 90°$ and $\tau = 45°$. The greater values of $N_r$represent thermal performance to thermal conduction through thermal radiation, while the lower value of N_r indicate heat conduction superiority. The domains of dynamical, thermodynamic, as well as diffusive boundary layers are quantitatively strengthened while N_r values grow. Actually, this may state as thermal diffusivity as well as the thermal radiation impact are similar. Figure 2a illustrates the effect of N_r upon momentum boundary layer flow of 2nd grade fluid over dual scenarios of concerning slants 90° and 45° by selecting appropriate constant values. These graphs demonstrate that the domain is pushed away from the sheet via expanding N_r. The Walters liquid B has a similar result. Figure 2b depicts the effects of N_r upon momentum, energy, also concentration kind of 2nd grade fluid over dual circumstances of inclined slants 90° and 45°. From these figures we concluded that convergence of fluid flow better as compared to absences of nanoparticles.

Figures 3a, b explain how the Richardson number (Λ) affects various features of 2nd grade fluid as couple circumstances of slants 90° and 45°, whereas other physical characteristics are assumed to be constant. Because $\Lambda > 0$ in these graphs, the buoyant force pushing on the accelerated sheet and promoting the fluid flow results inside the free convection flow. As a result, the convection factor has expanded, since boundary wall width should be governing over through the flow velocity, the flow field will be diminished. An effect on various profiles opposing to that of the above is identified for the decision $\Lambda \leq 0$. Therefore, the impact of Λ is the contrary of the consequence of N_r.

The significance of Hartmann number Q on axial velocity, temperature as well as concentration profiles is portrayed in Fig. 4 for two instances of an aligned angles 90° and 45°. With ongoing Qnumber growth, velocity temperature, and concentration distribution develops. The conclusion is shown in the picture, which indicates the result of the uniform transverse magnetic field. This assumption came from the fact that the injected uniform transverse MHD generates a resultant force like the Lorentz force, which results in an opposite response in the movement, enhancing the movement of profiles. The increase in the magnetic field Q allows the nanoparticles to conduct more heat, and hence an increase in velocity.

Figures 5–8 evaluate the impact of the mass transpiration component V_c as well as solution domain β upon stream zone besides additional physical factors held fixed for Walter's liquid B/2nd grade fluid with keeping the other parameter values at constant. Figures 5, 7 depict the consequences of second-grade fluid (positive K_1), although Figs. 6, 8 illustrate the effects of Walters' liquid B (negative K_1). Such graphs clearly show that for $K_1 = 0$, the stream and energy will each have a singular solution for all of the components, while solutions turn plenty for $K_1 < 0$ (complicated solution). Additionally, but such consequences vanish above the critical values specified by Eq. (23). Hence, it may be deduced that a range of solutions are possible with the suitable selection of the

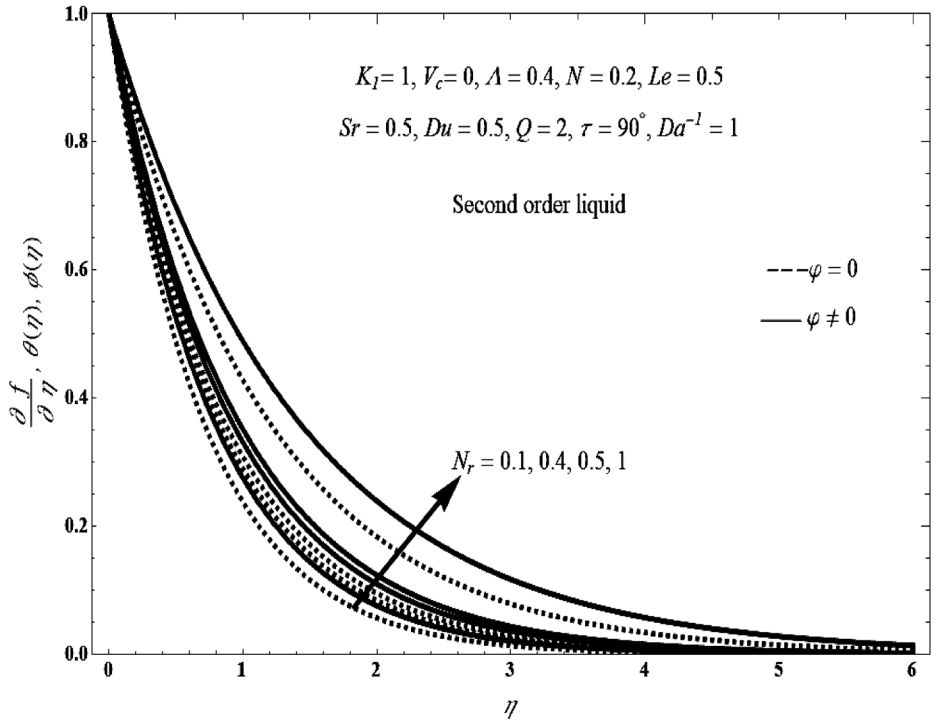

(a)

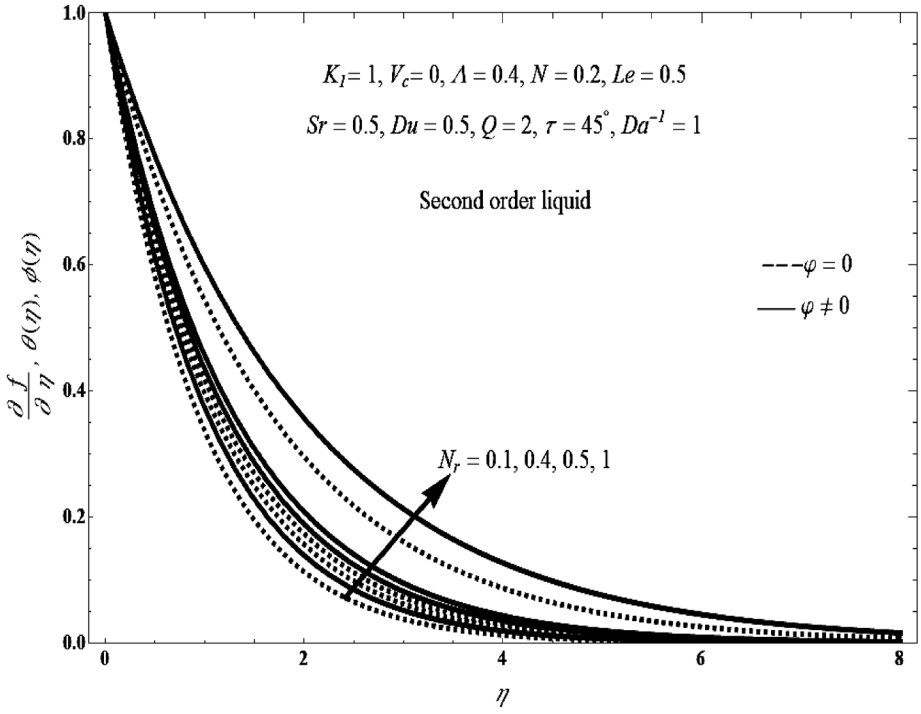

(b)

Fig. 2. An impact of N_r on $\frac{\partial f}{\partial \eta}$, $\theta(\eta)$, $\varphi(\eta)$ for (a) $\tau = 90^{\circ}$ and (b) $\tau = 45^{\circ}$.

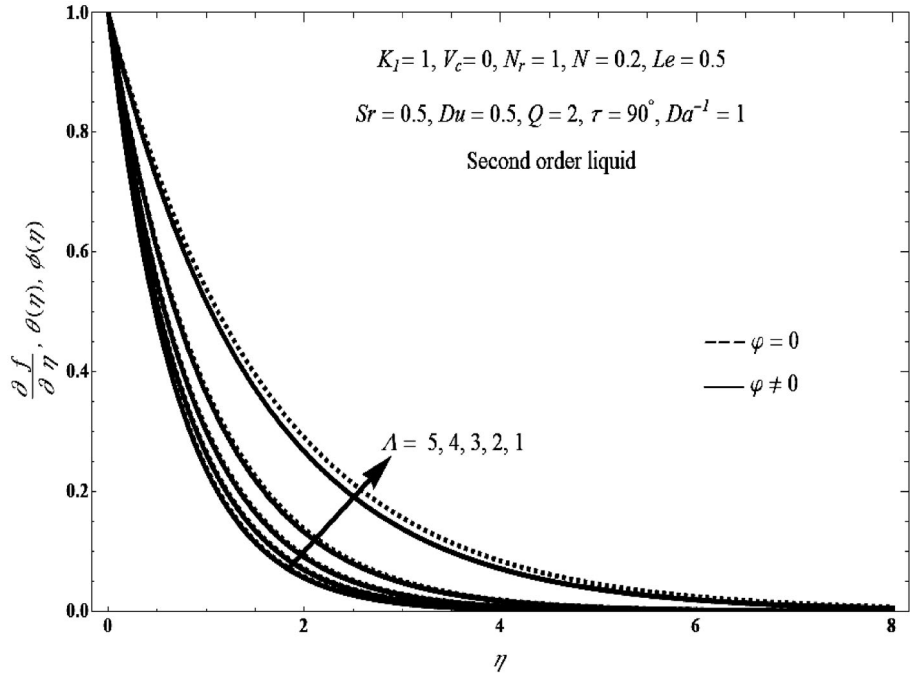

(a)

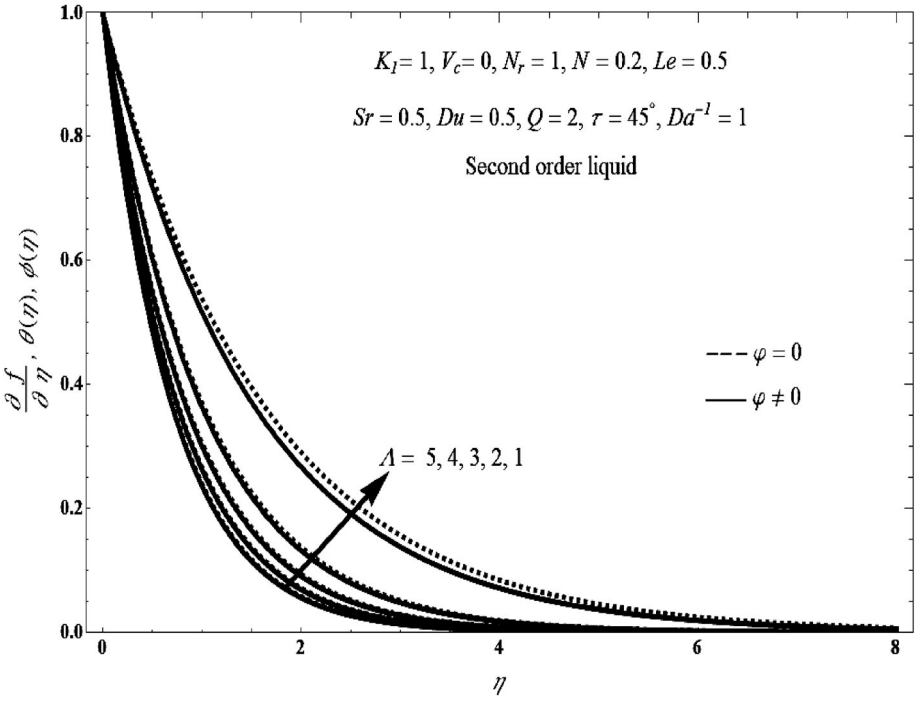

(b)

Fig. 3. An influence of Λ on $\frac{\partial f}{\partial \eta}$, $\theta(\eta)$, $\varphi(\eta)$ for (a) $\tau = 90^{\circ}$ and (b) $\tau = 45^{\circ}$.

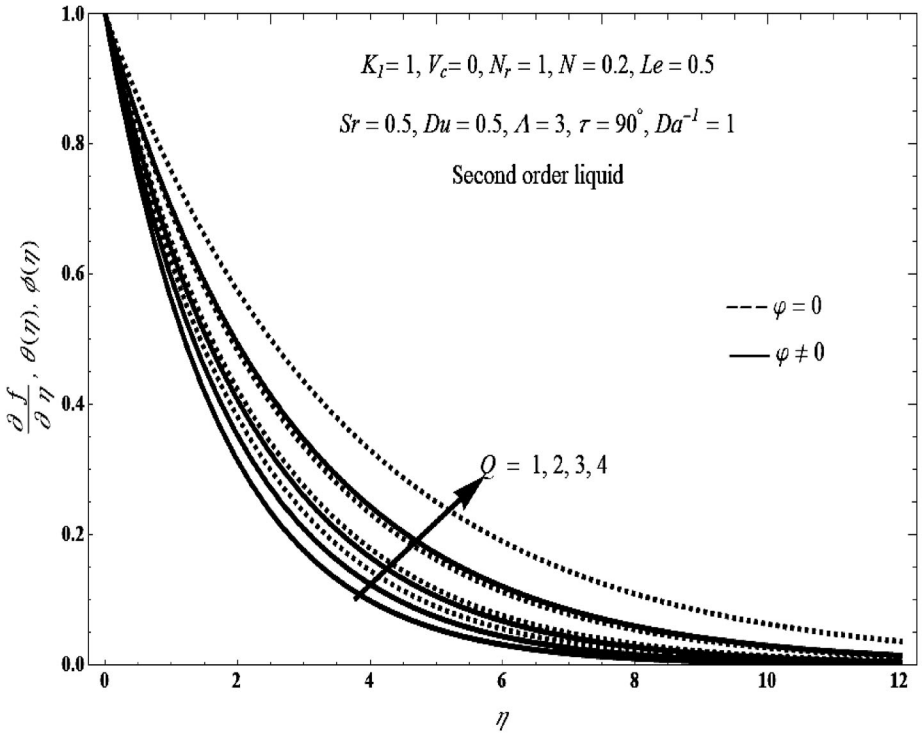

(a)

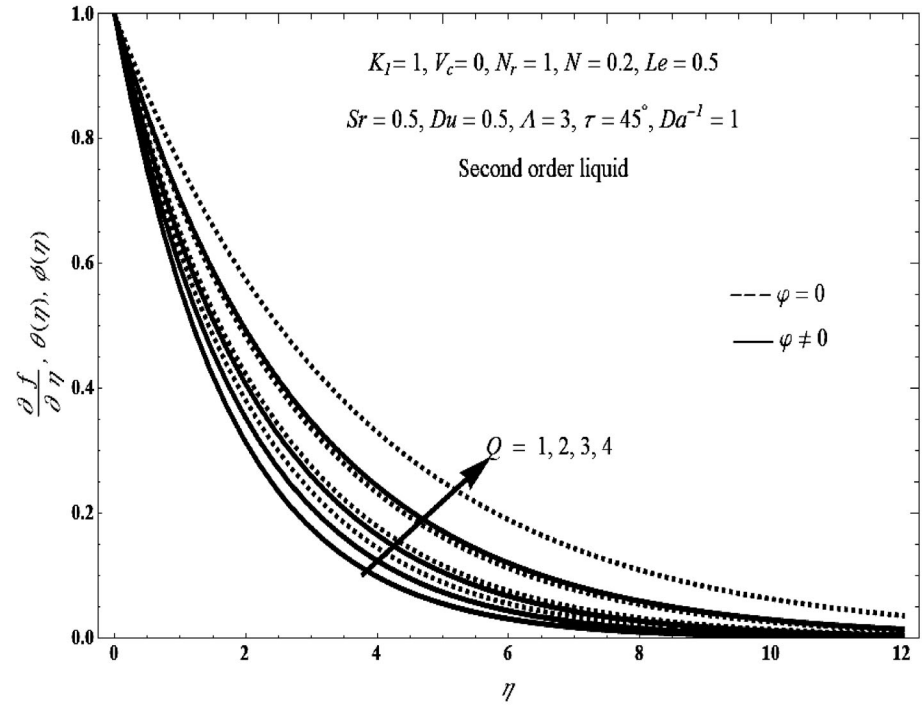

(b)

Fig. 4. An influence of Qon $\frac{\partial f}{\partial \eta}$, $\theta(\eta)$, $\varphi(\eta)$ for (a) $\tau = 90^\circ$ and (b) $\tau = 45^\circ$.

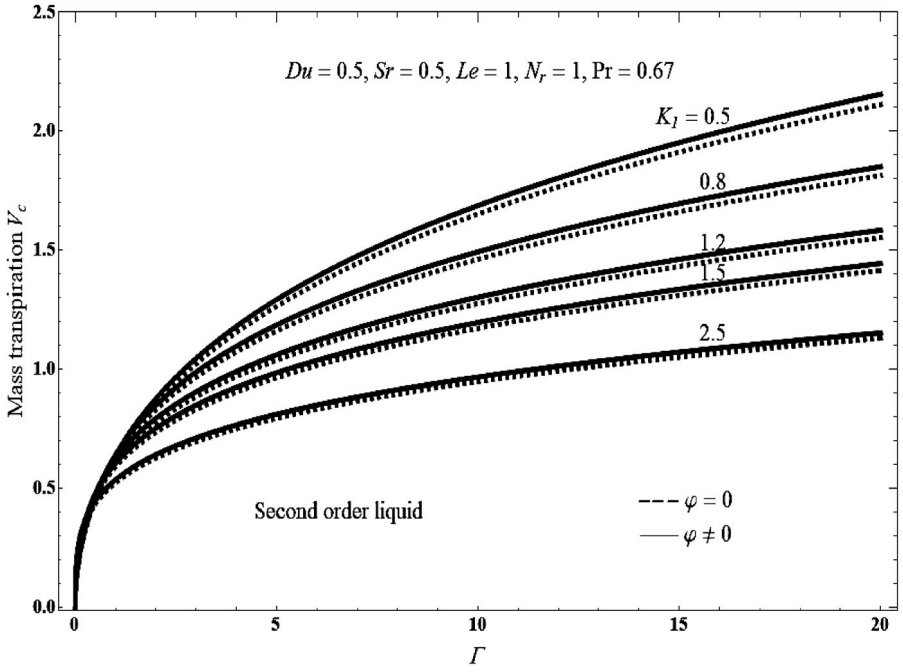

(a)

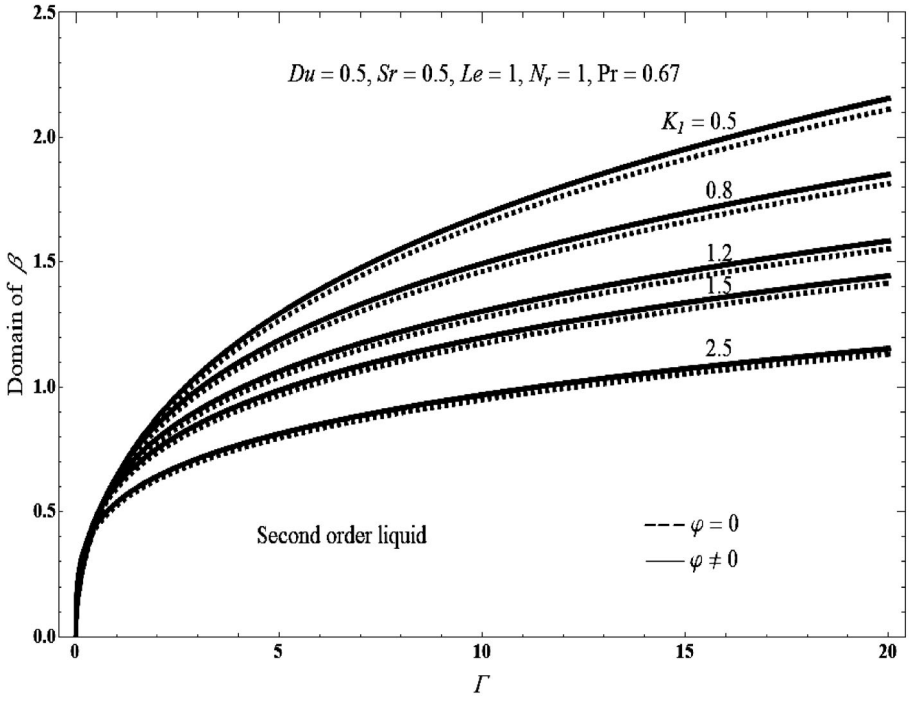

(b)

Fig. 5. Solution domain for (a) V_c against Γ and (b) β against Γ.

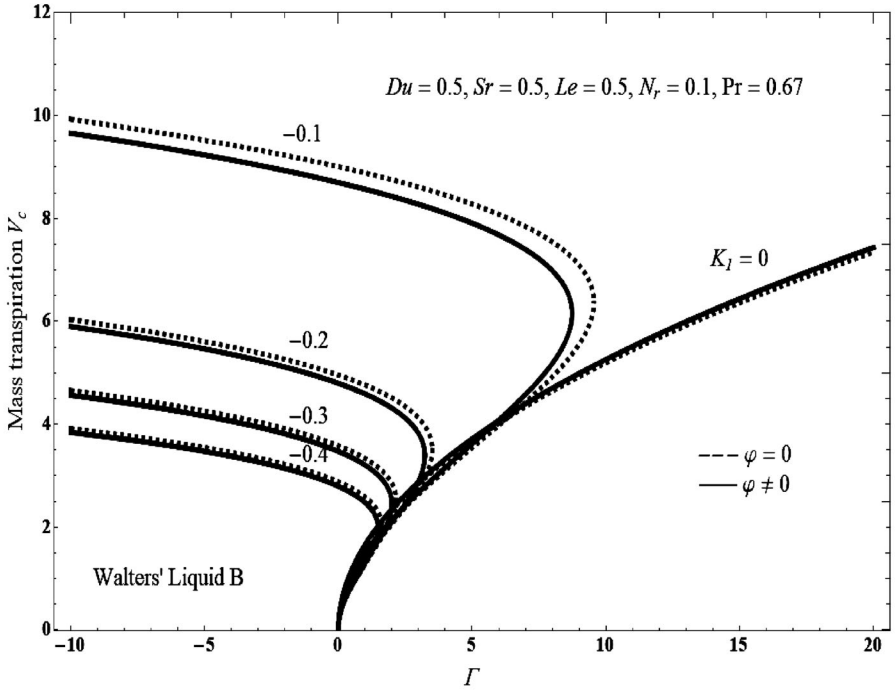

(a)

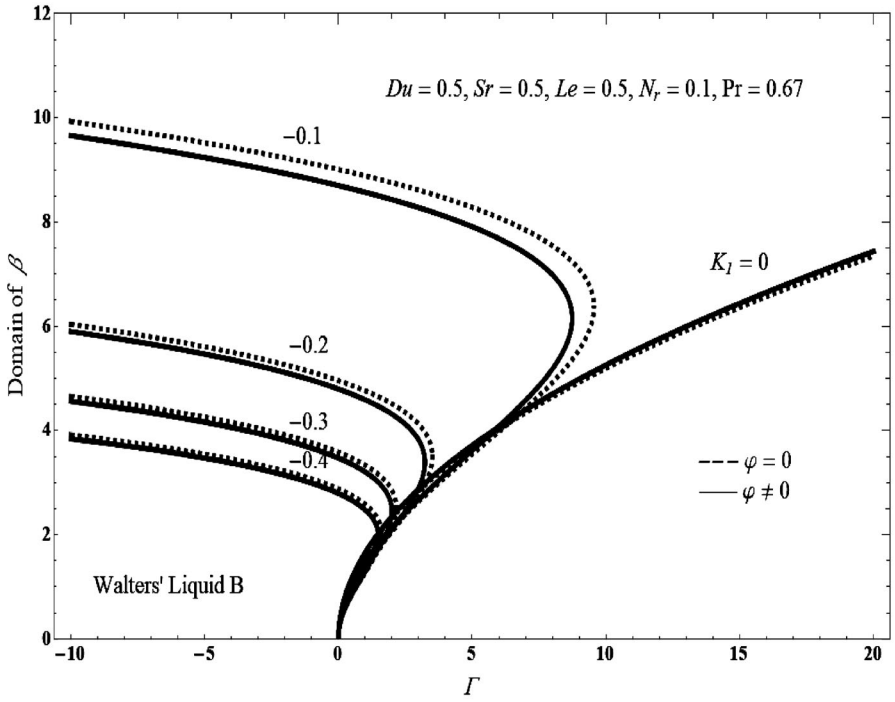

(b)

Fig. 6. Solution domain for (a) V_c against Γ and (b) β against Γ.

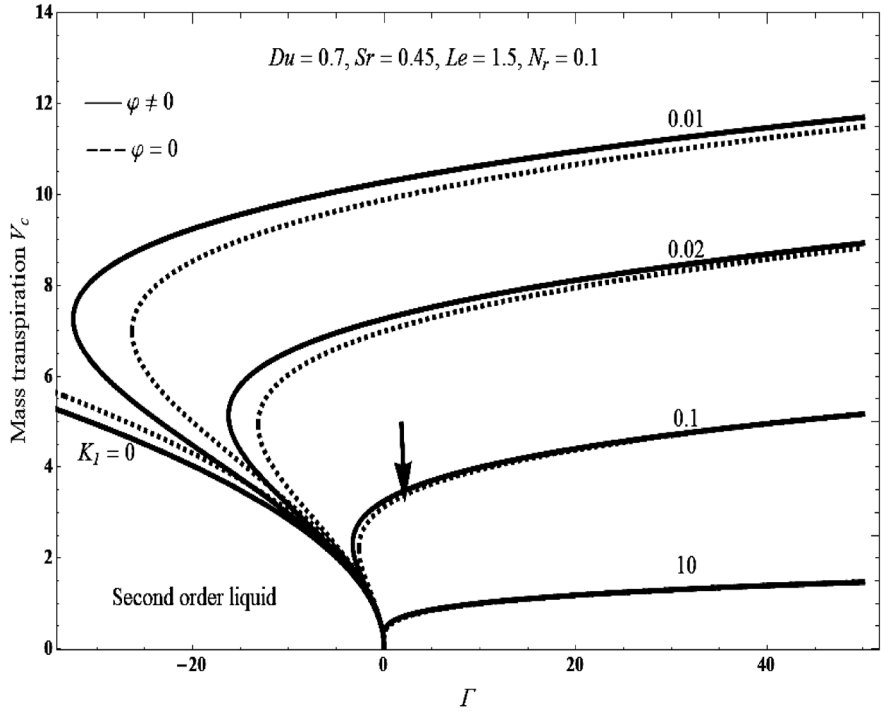

(a)

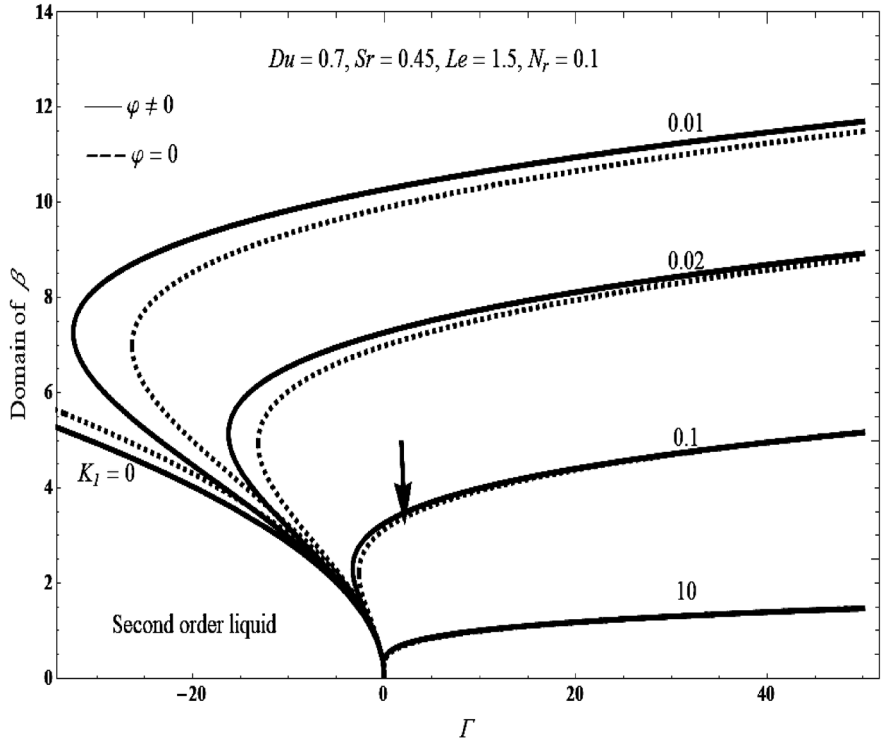

(b)

Fig. 7. Solution domain for (a) V_c against Γ and (b) β against Γ (for second order liquid with B).

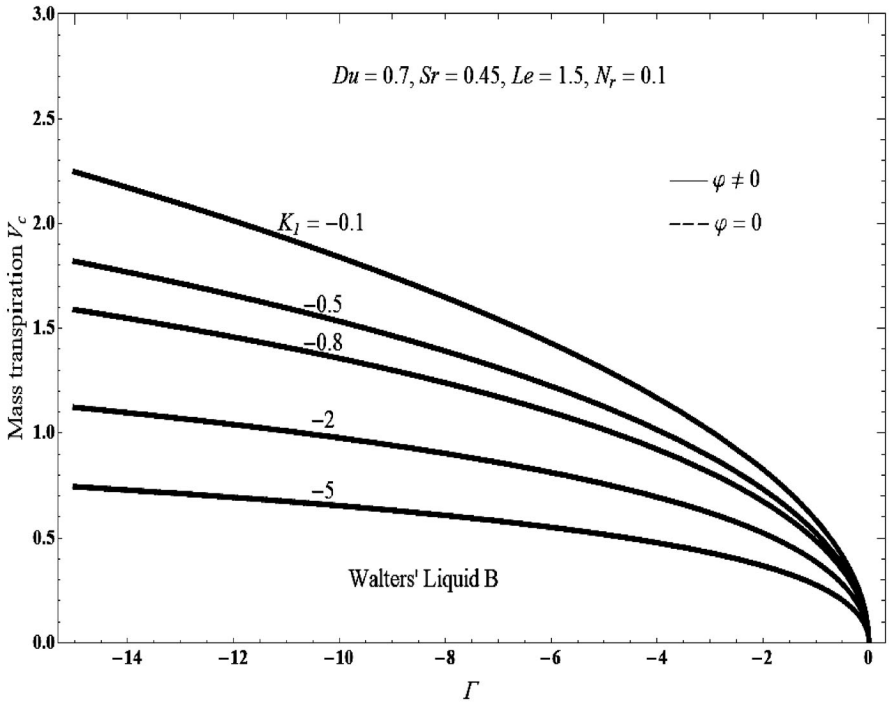

(a)

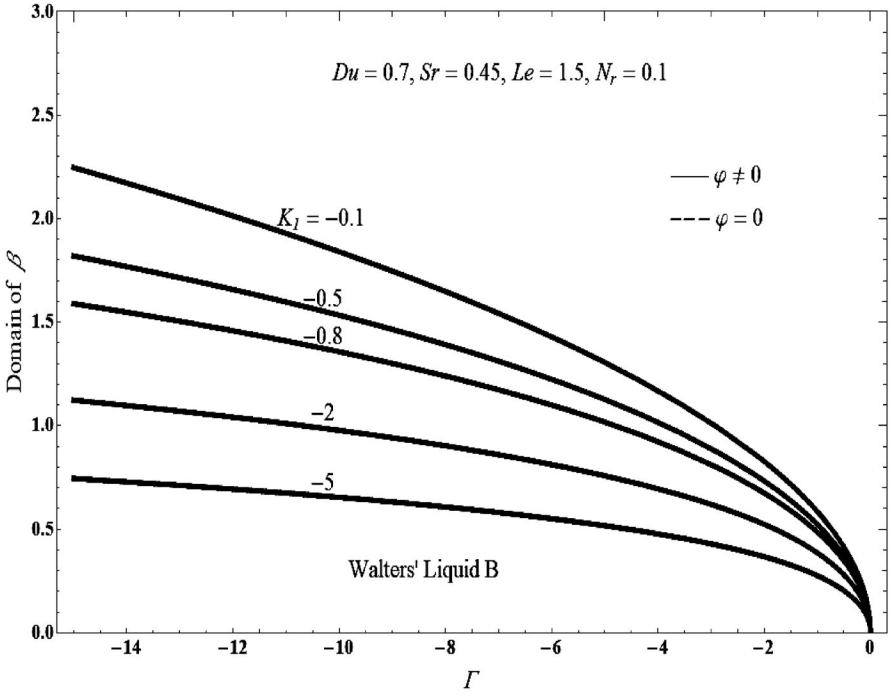

(b)

Fig. 8. Solution domain for (a) V_c against Γ and (b) β against Γ (for Walter's liquid B).

regulating physical parameters. Maintaining Pr as well as N_r steady, has the reverse effect on the flow pattern as the rapid development in the viscoelastic component does. The graphs of may display significant phenomena of β against $\Gamma = \Lambda\,(1+N) - \left(\frac{A_1}{A_2} Da^{-1} + \frac{A_3}{A_2} Q \sin^2 \tau\right)$.

5. CONCLUSIONS

In the present work, an effect of inclined MHD and radiation on mixed convective flow of viscoelastic flow past accelerating permeable surface with mass transpiration is explored analytically, the analytical solutions are received for the transformed equations. Analytical results for various values of physical application terms have been graphically portrayed and thoroughly analyzed. The present findings have been confirmed with the earlier reported studies [11, 25]. Following organization of the analytical solutions of relevant domains and optimization that takes into account 3D complexity, the key concepts can be stated as follows.

- As value of radiation upsurges slightly, the width of the velocity, as well as concentration boundary is enhanced.
- Richardson number increases, the thickness of the momentum, temperature with concentration boundary layer declines.
- Hartmann number improved with an enhancing the thickness of the momentum, temperature with concentration boundary layer.

Limiting case of the current study:

- $\lim\limits_{\tau=90^\circ,\,\varphi=0,\,N_r=0}$ {Results of our work} $\rightarrow$ {Results of Turkyilmazoglu [11]},
- $\lim\limits_{\varphi=0}$ {Results of our work} $\rightarrow$ {Results of Mahabaleshwar [21]}.

ABBREVIATIONS AND NOTATION

a—rate of acceleration (–)
b—constant (–)
B_0—magnetic field (Tesla)
c—constant (–)
C_s—susceptibility concentration (m^3/kg)
C_p—heat capacity ($JK^{-1}Kg^{-1}$)
Da^{-1}—inverse Darcy number (–)
D_m—diffusion of mass parameter (m^2/s)
D_f—Dufour number (–)
f—similarity function (–)
Gr_x—local Grashof number (–)
g—gravity acceleration (m/s^2)
K_T—ratio of thermal diffusion (m^2/s)
k^*—coefficient of mean absorption (cm^{-1})
k_0—constant of viscoelastic (–)
K_1—component of viscoelastic (–)
Le—Lewis number (–)
N—Buoyancy quantity (–)
N_r—radiation parameter (–)
Pr—prandtl number (–)
Q—Hartman number (–)
Re_x—Reynolds local number (–)
R_m—magnetic Reynolds number (–)

Sr—Soret number (–)
T—temperature of fluid (K)
T_m—mean fluid temperature (K)
U_w—accelerated velocity (m/s)
V_c—mass transpiration parameter (–)
v_w—mass flux velocity (m/s)
x—horizontal axis (–)
y—vertical axis (–)

Greek Symbols

β—constant (–)
β_T—thermal volume expansion parameter (–)
β_c—diffusive volume expansion coefficient (–)
η—similarity variable (–)
φ—concentration (–)
θ—temperature (–)
ν_m—magnetic permeability (N/A^2)
ρ_f—density (Kg·m^{-3})
σ_f—base fluid electrical conductivity (S/m)
σ^*—coefficient of Stefan–Boltzmann (–)
τ—inclined magnetic field (Tesla)
Γ—porous magneto-convection concentration parameter (–)

Subscripts

hnf—hybrid nanofluid (–)
w—wall situation (–)
∞—outside of the sheet (–)

Abbreviations

ODEs—ordinary differential equations (–)
PDEs—partial differential equations (–)
MHD—magnetohydrodynamic (–)

FUNDING

USM thanks the hospitality of Universidad de Tarapacá (Chile) in his research visiting scholar in which part of the manuscript was written. L.M.P. acknowledges financial support from the ANID through Convocatoria Nacional Subvención a Instalación en la Academia Convocatoria Año 2021, Grant SA77210040. LMP and DL acknowledges partial financial support from FONDECYT 1240985. T. Maranna would like to thank the financial assistance received from Karnataka Science and Technology Society (KSTePS) under the program of Karnataka DST-Ph.D fellowship for Science and Engineering: DST/KSTePS/Ph.D.Fellowship/MP-07:2023–24.

CONFLICT OF INTEREST

The authors of this work declare that they have no conflicts of interest.

REFERENCES

1. Choi, S.U. and Eastman, J.A., Enhancing Thermal Conductivity of Fluids with Nanoparticles, in *Procs. of the Int. Mechanical Engineering Congress and Exhibition*, San Francisco, CA, USA (1995), pp. 12–17.
2. Alharbi, F.M., Naeem, M., Zubair, M., Jawad, M., Jan, W.U., and Jan, R., Biconvection due to Gyrotactic Microorganisms in Couple Stress Hybrid Nanofluid Laminar Mixed Convection Incompressible Flow with Magnetic Nanoparticle and Chemical Reaction as Carrier for Targeted Drug Delivery through Porous Stretching Sheet, *Molecules*, 2021, vol. 26, no. 13, p. 3954.
3. Verma, S.K., Tiwari, A.K., Tiwari, S., and Chauhan, D.S., Performance Analysis of Hybrid Nanofluids in Flat Plate Solar Collector as an Advanced Working Fluid, *Solar Energy*, 2018, vol. 167, pp. 231–241.
4. Sarkar, J., Ghosh, P., and Adil, A., A Review on Hybrid Nanofluids: Recent Research, Development and Applications, *Renew. Sust. Energ. Rev.*, 2015, vol. 43, pp. 164–177.
5. Devi, S.P.A. and Uma devi, S.S., Numerical Investigation of Hydromagnetic Flow over a Permeable Stretching Sheet with Suction, *Int. J. Nonlin. Sci. Numer. Simul.*, 2016, vol. 17, no. 5, pp. 249–257.
6. Mahabaleshwar, U.S., Vishalakshi, A.B., and Anderson, H.I., Hybrid Nanofluid Flow past a Stretching/Shrinking Sheet with Thermal Radiation and Mass Transpiration, *Chinese J. Phys.*, 2022, vol. 75, pp. 152–168.
7. Sneha, K.N., Mahabaleshwar, U.S., and Bhattacharyya, S., An Effect of the Thermal Radiation on Inclined MHD Flow in Hybrid Nanofluids over a Stretching/Shrinking Sheet, *J. Therm. An. Calorim.*, 2022, pp. 1–15.
8. Mahabaleshwar, U.S., Aly, E.H., and Anusha, T., MHD Slip Flow of a Casson Hybrid Nanofluid over a Stretching/Shrinking Sheet with Thermal Radiation, *Chinese J. Phys.*, 2022, vol. 80, pp. 74–106.
9. Mahabaleshwar, U.S., Anusha, T., and Hatami, M., The MHD Newtonian Hybrid Nanofluid Flow and Mass Transfer Analysis due to Super-Linear Stretching Sheet Embedded in Porous Medium, *Sci. Rep.*, 2021, vol. 11, no. 1, pp. 1–17.
10. Anusha, T., Huang, H.N., and Mahabaleshwar, U.S., Two Dimensional Unsteady Stagnation Point Flow of a Casson Hybrid Nanofluid over a Permeable Flat Surface and Heat Transfer Analysis with Radiation. *J. Taiwan Inst. Chem. Eng.*, 2021, vol. 12, pp. 79–91.
11. Turkyilmazoglu, M., The Analytical Solution of Mixed Convection Flow Heat Transfer and Fluid Flow of a MHD Viscoelastic Fluid over a Permeable Stretching Surface, *Int. J. Mech. Sci.*, 2013, vol. 77, pp. 263–268.
12. Mukhopadhyay, S., Effect of Thermal Radiation on Unsteady Mixed Convection Flow and Heat Transfer over a Porous Stretching Surface in Porous Medium, *Int. J. Heat Mass Transfer*, 2009, vol. 52, pp. 3261–3265.
13. Ferdows, M., Adesanya, S.O., and Alzahrani, F., Numerical Investigation of a Boundary Layer Water-Based Nanofluid Flow with Induced Magnetic Field, *Phya Stat. Mech. Appl.*, 2021, vol. 570, p. 125492.
14. Waini, I., Ishak, A., and Pop, I., Mixed Convection Flow over an Exponentially Stretching/Shrinking Vertical Surface in a Hybrid Nanofluid, *Alex. Eng. J.*, 2020, vol. 59, no. 3, pp. 1881–1891.
15. Khan, U., Waini, I., Zaib, A., Ishak, A., and Pop, I., MHD Mixed Convection Hybrid Nanofluids Flow over a Permeable Moving Inclined Flat Plate in the Presence Thermophoretic and Radiative Heat Flux Effects, *Mathematics*, 2022, vol. 10, p. 1164.
16. Ashraf, M.B., Hayat, T., and Alsaedi, A., Mixed Convection Flow of Casson Fluid over a Stretching Sheet with Convective Boundary Conditions and Hall Effect, *Bound. Value Probl.*, 2017, vol. 137, pp. 1–7.
17. Metri, P.G., Metri, P.G., Abel, S., and Silvestrov, S., Heat Transfer in MHD Mixed Convection Viscoelastic Fluid Flow over a Stretching Sheet Embedded in a Porous Medium with Viscous Dissipation and Non-Uniform Heat Source/Sink, *Procedia Eng.*, 2016, vol. 157, pp. 309–316.
18. Ramesh, G.K., Gireesh, B.J., and Chamkha, A.J., MHD Mixed Convection Flow of Viscoelastic Fluid over an Inclined Surface with a Non-Uniform Heat Source/Sink, *Can. J. Phys.*, 2013, vol. 91, pp. 1074–1080.
19. Singh, J.K., Seth, G.S., Vishwanath, S., and Rohidas, P., Steady MHD Mixed Convection Flow of a Viscoelastic Fluid over a Magnetized Convectively Heated Vertical Surface with Hall Current and Induced Magnetic Field Effects, *Heat Transfer*, 2020, vol. 49, pp. 1–24.
20. Gamachu, D. and Ibrahim, W., Mixed Convection Flow of Viscoelastic Ag–Al_2O_3/Water Hybrid Nanofluid past a Rotating Disk, *Phys. Scr.*, 2021, vol. 9, p. 125205.
21. Mahabaleshwar, U.S., Nagaraju, K.R., Kumar, P.N.V., Nadagoud, M.N., Bennacer, R., and Sheremet, M.A., Effects of Dufour and Soret Mechanism on MHD Mixed Convective-Radiative Non-Newtonian Liquid Flow and Heat Transfer over a Porous Sheet, *Therm. Sci. Eng. Prog.*, 2020, vol. 16, p. 100459.
22. Maranna, T., Sneha, K.N., Mahabaleshwar, U.S., Sarris, I.E., and Karakasidis, T.E., An Effect of Radiation and MHD Newtonian Fluid over a Stretching/Shrinking Sheet with CNTs and Mass Transpiration, *Appl. Sci.*, 2022, vol. 12, p. 5466.
23. Vishalakshi, A.B., Maranna, T., Mahabaleshwar, U.S., and Laroze, D., An Effect of MHD on Non-Newtonian Fluid Flow over a Porous Stretching/Shrinking Sheet with Heat Transfer, *Appl. Sci.*, 2022, vol. 12, p. 4937.

24. Mahabaleshwar, U.S., Maranna, T., and Sofos, F., Analytical Investigation of an Incompressible Viscous Laminar Casson Fluid Flow past a Stretching/Shrinking Sheet, *Sci. Rep.*, 2022, vol. 12, p. 18404.
25. Kumar, M.A., Reddy, Y.D., Rao, V.S., and Goud, B.S., Thermal Radiation Impact on MHD Heat Transfer Natural Convective Nanofluid Flow over an Impulsively Started Verticle Plate, *Case Stud. Therm. Eng.*, 2021, vol. 24, p. 100826.
26. Asghar, A., Lund, L.A., Shah, Z., Vrinceanu, N., Deebani, W., and Shutaywi, M., Effect of Thermal Radiation on Three-Dimensional Magnetized Rotating Flow of Hybrid Nanofluid, *Nanomat.*, 2022, vol. 12, p. 1566.
27. Waini, I., Ishak, A., and Pop, I., Magnetohydrodynamic Flow past a Shrinking Vertical Sheet in a Dusty Hybrid Nanofluid with Thermal Radiation. *Appl. Math. Mech.–Engl. Ed.*, 2022, vol. 43, pp. 127–140.
28. Nadeem, M., Siddique, I., and Awrejcewicz, J., Numerical Analysis of a Second-Grade Fuzzy Hybrid Nanofluid Flow and Heat Transfer over a Permeable Stretching/Shrinking Sheet, *Sci. Rep.*, 2022, vol. 12, p. 1631.
29. Roy, N.C. and Pop, I., Flow and Heat Transfer of a Second-Grade Hybrid Nanofluid over a Permeable Stretching/Shrinking Sheet, *Eur. Phys. J. Plus*, 2020, vol. 135, p. 768.
30. Ghalambaz, M., Roşca, N.C., Roşca, A.V., Pop, I., Ros, N.C., Ros, A.V., and Pop, I., Mixed Convection and Stability Analysis of Stagnation-Point Boundary Layer Flow and Heat Transfer of Hybrid Nanofluids over a Vertical Plate, *Int. J. Numer., Methods Heat Fluid Flow*, 2019, vol. 30, pp. 3737–3754.
31. Nada, E.A. and Oztop, H.F., Effects of Inclination Angle on Natural Convection in Enclosures Filled with Cu–Water Nanofluid, *Int. J. Heat Fluid Flow*, 2009, vol. 30, pp. 669–678.
32. Yashkun, U., Zaimi, K., Ishak, A., Pop, I., and Sidaoui, R., Hybrid Nanofluid Flow through an Exponentially Stretching/Shrinking Sheet with Mixed Convection and Joule Heating, *Int. J. Numer. Methods Heat Fluid Flow*, 2020, vol. 31, pp. 1930–1950.
33. Oztop H.F. and Nada, E.A., Numerical Study of Natural Convection in Partially Heated Rectangular Enclosures Filled with Nanofluids, *Int. J. Heat Fluid Flow*, 2008, vol. 29, pp. 1326–1336.